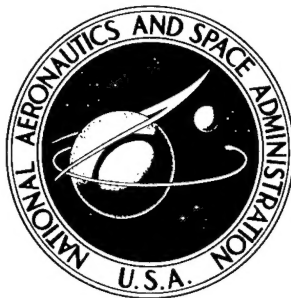


NASA TECHNICAL NOTE

NASA TN D-2768



NASA TN D-2768

AMPTIAC

60064

(THE TERNARY SYSTEM
TANTALUM-HAFNIUM-CARBON
AT 2050° C) *jlz*

Reproduced From
Best Available Copy

by Daniel L. Deadmore and Isidor Zaplatynsky

Lewis Research Center
Cleveland, Ohio

20011210 072

NATIONAL AERONAUTICS AND SPACE ADMINISTRATION • WASHINGTON, D. C. • APRIL 1965

NASA TN D-2768

THE TERNARY SYSTEM TANTALUM-HAFNIUM-CARBON AT 2050° C

By Daniel L. Deadmore and Isidor Zaplatynsky

Lewis Research Center
Cleveland, Ohio

NATIONAL AERONAUTICS AND SPACE ADMINISTRATION

For sale by the Clearinghouse for Federal Scientific and Technical Information
Springfield, Virginia 22151 – Price \$1.00

THE TERNARY SYSTEM TANTALUM-HAFNIUM-CARBON AT 2050° C

by Daniel L. Deadmore and Isidor Zaplatynsky

Lewis Research Center

SUMMARY

An isothermal cross section of the tantalum-hafnium-carbon (Ta-Hf-C) system at 2050° C was constructed from x-ray diffraction, chemical analysis, metallographic, and microhardness data. No phases other than those appearing in the three binary systems were observed in the ternary system. A liquid phase was found in a large portion of the hafnium-rich corner of the ternary section.

INTRODUCTION

The melting points of tantalum carbide (TaC) and hafnium carbide (HfC) are very high ($\approx 3950^{\circ}$ and 3900° C, respectively) and the 4-tantalum-carbide - hafnium-carbide ($4 \text{ TaC} \cdot \text{HfC}$) solid solution is a material of the highest known melting point ($\approx 4100^{\circ}$ C) (ref. 1). Therefore, compositions within the TaC-HfC pseudobinary system are considered for possible application in the field of high-temperature thermionic energy conversion. In this connection vaporization studies have been conducted (ref. 2) in order to establish the thermal stability of TaC-HfC solid solutions. In the course of that investigation it was observed that compositional changes occurred on the surface of these carbides due to differences in the vaporization rates of tantalum (Ta), hafnium (Hf), and carbon (C). Consequently, a need became apparent for the knowledge of ternary equilibrium phase relations. An experimental study was initiated to determine the ternary diagram at 2050° C. This temperature was chosen because it is within the range of possible thermionic emitter operation. While the present work was in progress, an isothermal section of this system at 1850° C was reported (ref. 3).

Previous literature related to the present work includes binary diagrams for Ta-C (ref. 4), Hf-C (ref. 5), Ta-Hf (ref. 6), and ternary phase relations of Ta-Hf-C at 1850° C (ref. 3). These are shown in figure 1.

In the investigation reported here, the isothermal section at 2050° C of the Ta-Hf-C system was determined. Samples were prepared by several powder-metallurgical techniques and by arc melting. After homogenization heat treatment at 2050° C in vacuum, samples were rapidly cooled, and phase identification was made by x-ray diffraction, metallographic, and microhardness techniques.

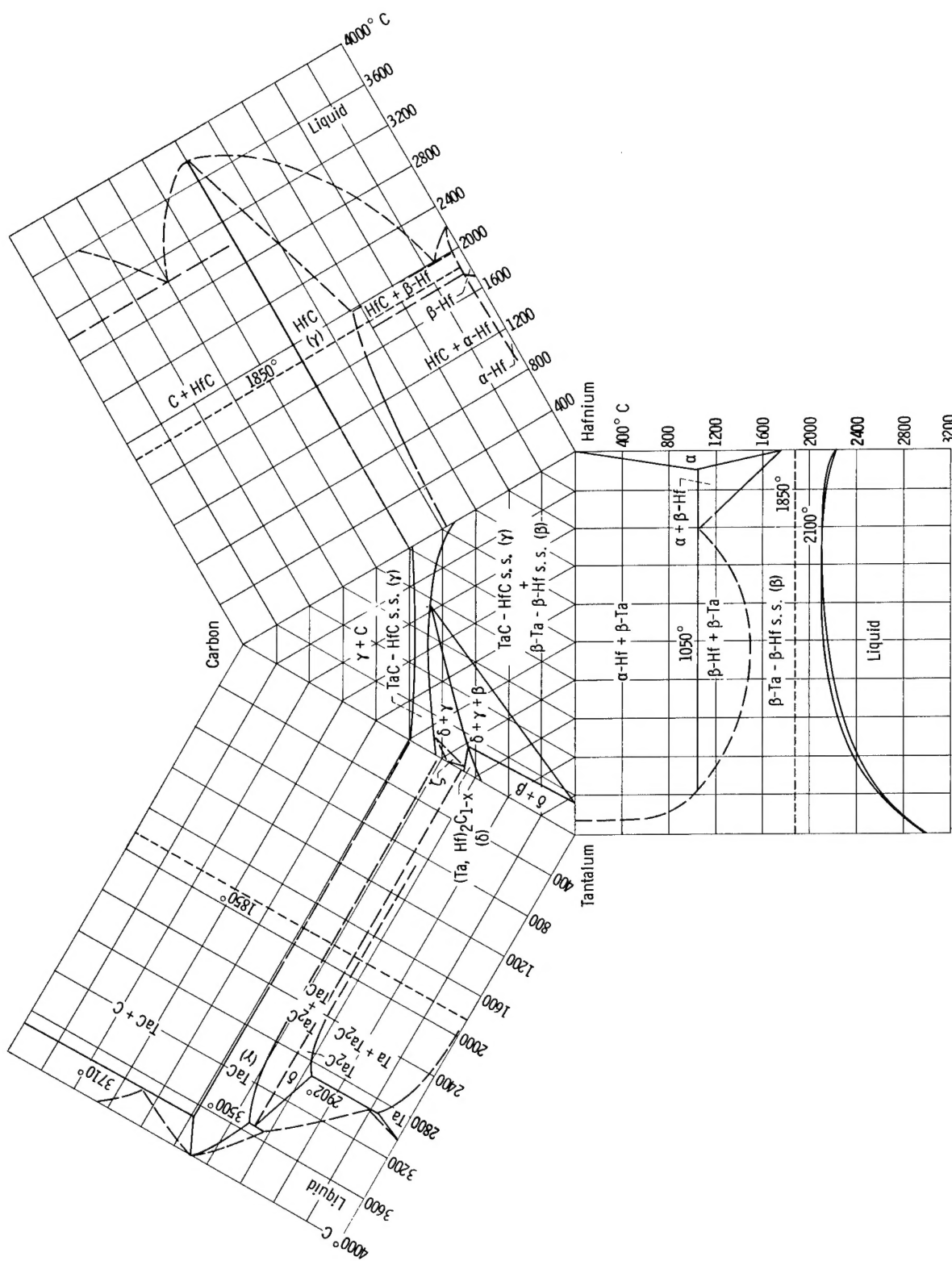


Figure 1. - Binary and ternary tantalum-hafnium-carbon systems given in literature. Ternary system is isothermal section at 1850° C.

EXPERIMENTAL PROCEDURE

Sample Preparation

The starting materials used in the preparation of the samples were tantalum hydride (TaH), hafnium-hydride (HfH₂), and spectrographic grade carbon. The analyses of the hydrides are given in table I.

Samples were prepared by three techniques: (1) sintering of cold-pressed mixtures, (2) hot pressing, and (3) sintering followed by arc melting. The cold-pressed and sintered specimens were prepared by blending the required amounts of the component powders followed by hydrostatically compacting (85 000 psi) at room temperature without a binder. These compacts, contained within thorium oxide crucibles, were set inside a tungsten susceptor and were slowly heated by induction in a vacuum of 5×10^{-6} to 9×10^{-6} torr to avoid rapid evolution of hydrogen. The specimens were brought up to 2050° C and held at that temperature for periods of from 1 to 30 hours until reaction was complete. The specimens were then cooled at a rate of 1000° C per minute to 900° C then more slowly to room temperature. The extent of reaction was determined by x-ray diffraction examination after each 1 to 5 hours of heating. Completion of reaction was assumed when the diffraction pattern showed no change. Several samples were checked for thorium content with an alpha counter. No thorium pickup was indicated.

Some compositions in the pseudobinary TaC-HfC region (about 50 atomic percent C) were hot pressed in graphite dies at 2400° to 2700° C at 3200 pounds per square inch for 1/2 to 1 hour.

Selected compositions were arc melted in argon using a nonconsumable tungsten electrode and a water-cooled copper hearth. The pickup of tungsten by the samples determined by chemical analysis was 0.01 to 0.1 weight percent.

All the hot-pressed and arc-melted samples were heat treated at 2050° C in vacuum for times up to 30 hours and cooled at a rate of 1000° C per minute to 900° C then more slowly to room temperature. This cooling rate is believed to be sufficiently rapid to retain the high-temperature phases except in hafnium-rich compositions where the precipitation of α -hafnium was observed. Even considerably faster cooling of composition 86 did not arrest the formation of α -hafnium. All sample compositions, along with phases present at room temperature, are given in table II.

It was also observed that sintered compositions 83, 85, 86, 87, 88 and 89, in the hafnium-rich corner of the diagram, showed large shrinkages, some deformation, and greatly increased densities. These observations suggest the presence of a liquid phase at 2050° C.

Measurements

Since it was expected that carbon loss would occur during preparation and heat treatment, all final products were analyzed for total and free carbon and the final composition calculated accordingly.

Temperature determinations were made with a disappearing-filament-type micro-optical pyrometer calibrated against a standard tungsten strip lamp (including the optical prism, which was part of the furnace). Temperature was determined with an accuracy of $\pm 30^{\circ}$ C.

A room-temperature x-ray diffraction study was done on powdered samples (taken from the center of the specimens) with nickel-filtered copper radiation using a diffractometer. In the case of metal-phase-rich compositions, which could not be easily ground, the patterns were taken from the interior cross section of the specimen. The lines on each pattern were indexed without difficulty because the structures of the phases involved were cubic or hexagonal. Lattice parameters were calculated on a 7094 computer by the least-squares method using the $1/\sin^2\theta$ extrapolation function. The standard deviation of all lattice parameters was ± 0.005 angstrom.

All arc-melted and some of the sintered compositions were examined by a metallographic technique. Etching was done with a mixture of hydrofluoric acid, nitric acid, and water. The composition of the etchant varied from one sample to another. When possible, the Knoop microhardness of the phases was determined with a 50-gram load. The hardness numbers reported are the average of 15 indentations. The standard deviation is ± 10 percent of the reported value.

RESULTS

X-ray Diffraction Study

The examination of the x-ray patterns revealed that no phases were present other than those appearing in the three binary systems. These are the face-centered-cubic $\gamma(\text{Ta},\text{Hf})\text{C}_{1-x}$, hexagonal $\delta(\text{Ta},\text{Hf})_2\text{C}_{1-x}$, hexagonal $\alpha(\text{Hf},\text{Ta})$, and body-centered-cubic $\beta(\text{Ta},\text{Hf})$ phases. Of course, the lattice parameters of these phases changed with the composition. This change was particularly large in the case of the TaC-HfC solid solution. The number and identity of the phases in each composition were determined as shown in figure 2. Each composition is identified by its sample number (composition). The same information is tabulated in table II, where, in addition to the number and identity of the phases, the lattice parameters are listed. Since x-ray diffraction patterns were taken at room temperature, the Ta-Hf body-centered-cubic solid solutions in the hafnium-rich corner were in some cases not observed, but instead body-centered-cubic tantalum and the hexagonal form of hafnium were detected. However, it is known from the binary Ta-Hf system that at 2050° C there is only one phase present, the $\beta(\text{Ta},\text{Hf})$ body-centered-cubic solid solution. In some instances when a phase was detected, but there were not enough diffraction lines for accurate determination of the lattice parameter, only its presence was indicated (table II). Since TaC-HfC solid solutions are of considerable practical interest because of their high melting points, their lattice parameters are shown as a function of composition in figure 3. The iso-lattice parameter lines are also drawn with the aid of data taken from references 3, 7, and 8.

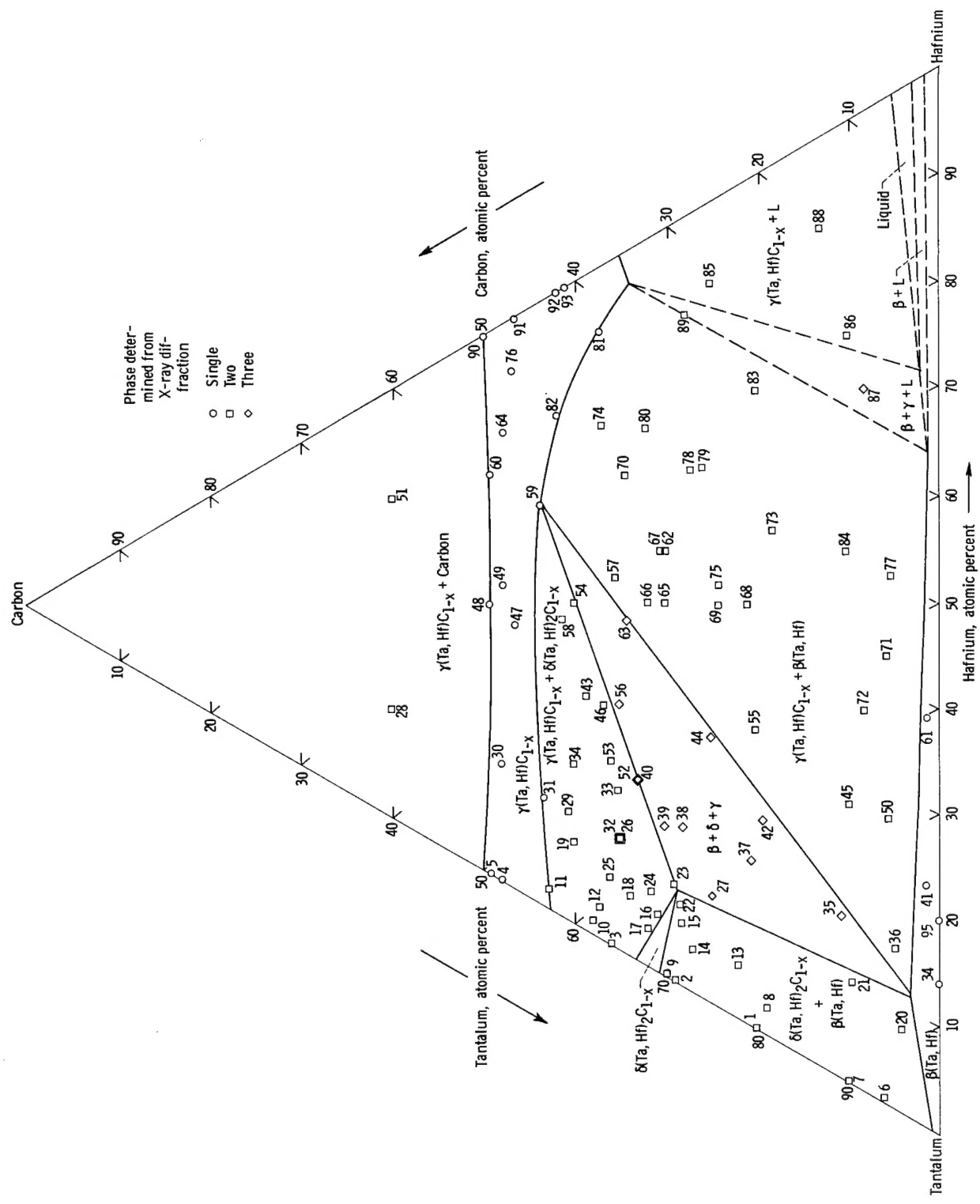


Figure 2 - Proposed isothermal cross section of tantalum-hafnium-carbon system at 2050°C.

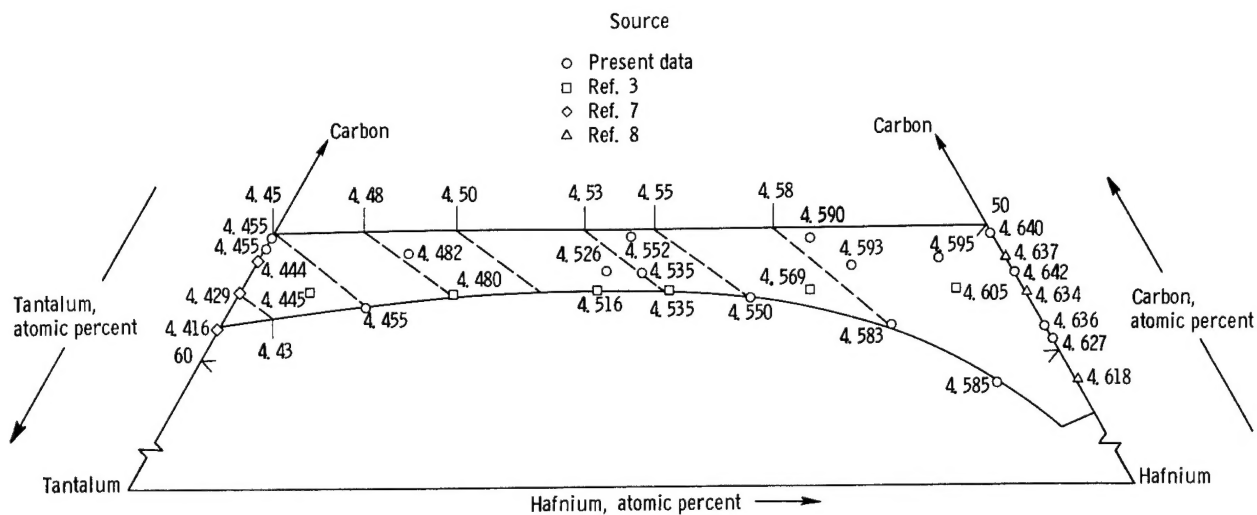


Figure 3. - Lattice parameters in face-centered-cubic (γ) single-phase region of tantalum-hafnium-carbon system.

Metallography

The sintered samples containing only small amounts of metallic phase were porous and could not be prepared for metallographic examination. The sintered samples, which contained a significant amount of metallic phase, and the samples which were arc melted, were mounted and polished with diamond compound.

There is agreement between results obtained from metallography and x-ray investigation concerning the number of phases present in a given sample. Representative microstructures of sintered and arc-melted samples are shown in figure 4. The numbers in parentheses indicate the content of Ta, Hf, and C, respectively, in atomic percent. The phases are labeled and their microhardness (Knoop Hardness Number (KHN)) noted.

Figure 4(a), composition 48, is a typical microstructure of compositions in the region of the TaC-HfC pseudobinary system. With the exception of a few black areas, possibly due to porosity, impurities, or free carbon, only the γ -phase $(\text{Ta},\text{Hf})\text{C}_{1-x}$ (with nearly maximum carbon content) is present.

The structure shown in figure 4(b) is typical of the $\gamma(\text{Ta},\text{Hf})\text{C}_{1-x}$ + carbon phase field. Here completely carbon-saturated grains of γ -phase are found surrounded by carbon.

Composition 34, shown in figure 4(c), is typical of the $\gamma(\text{Ta},\text{Hf})\text{C}_{1-x} + \delta(\text{Ta},\text{Hf})_2\text{C}_{1-x}$ phase field. The major component is the striated γ -phase. Similar striated structures have been observed in Ta-C binary compositions and reference 9 suggests these are the result of Ta_2C precipitation. The non-striated, intergranular component is the lower melting δ -phase.

Composition 44, within the three-phase area, yields a quite indiscernible microstructure, as shown in figure 4(d). The light areas are probably

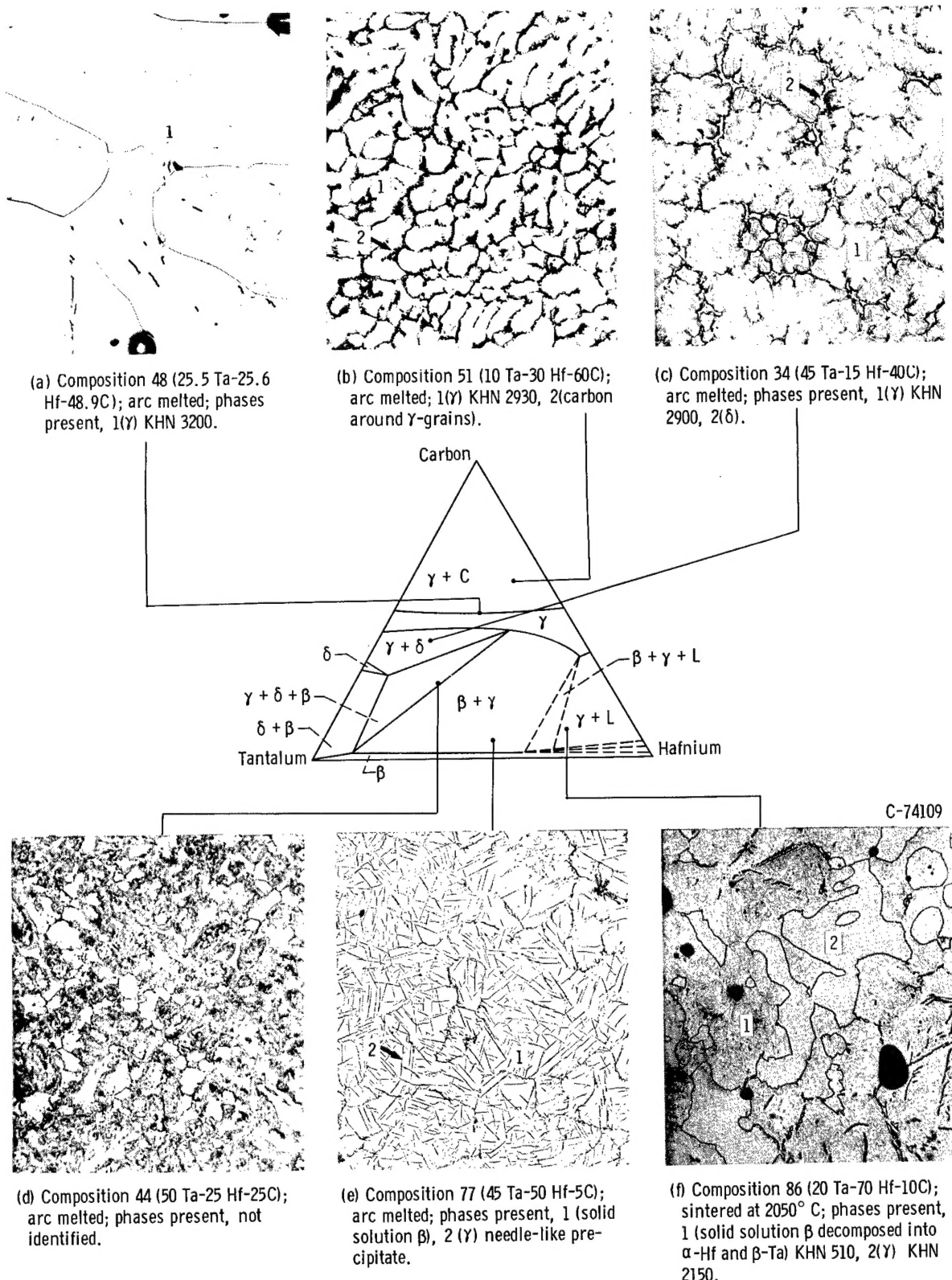


Figure 4. - Typical microstructures in tantalum-hafnium-carbon system. X250. Reduced 45 percent in printing.

γ -phase $(\text{Ta},\text{Hf})\text{C}_{1-x}$. An x-ray diffraction pattern taken from the sample revealed the presence of three phases, $\gamma(\text{Ta},\text{Hf})\text{C}_{1-x}$, $\delta(\text{Ta},\text{Hf})_2\text{C}_{1-x}$, and $\beta(\text{Ta},\text{Hf})$.

The two-phase $\gamma(\text{Ta},\text{Hf})\text{C}_{1-x} + \beta(\text{Ta},\text{Hf})$ equilibrium area is represented in figure 4(e). The matrix is mostly β -phase, (Ta,Hf) , with a needle-like precipitate of γ -phase, $(\text{Ta},\text{Hf})\text{C}_{1-x}$. Here one would expect to see an α -hafnium phase as a result of the decomposition of $\beta(\text{Ta},\text{Hf})$ solid solution (at 2050° C) on cooling. This was not the case, however, and the absence of α -hafnium was also verified by the x-ray diffraction method.

The photomicrograph of composition 86 is shown in figure 4(f). The metallic phase, which was liquid at 2050° C, yielded, on cooling, a mixture of α -Hf and β -Ta. The γ -phase, $(\text{Ta},\text{Hf})\text{C}_{1-x}$, forms large grains of irregular shape surrounded by the fine-textured α -Hf + β -Ta mixture. After heat treatment at 2050° C this specimen was deformed as a result of the presence of a liquid phase.

Microhardness

Microhardness information from references 10 to 12 as well as present data are shown in figure 5. The Knoop hardness values for the γ -phase, $(\text{Ta},\text{Hf})\text{C}_{1-x}$, vary from 1100 kilograms per square millimeter for carbon-deficient TaC to 3720 kilograms per square millimeter, when the hafnium content reaches about 11 atomic percent and the carbon is 48 atomic percent. Further increase in hafnium content, while approximately the same carbon content is maintained, causes a decrease in hardness. Completely carburized γ -phase compositions, in particular $\text{TaC}_{1.0}$, are significantly softer than carbon-deficient compositions. Figure 5 also shows that the hardness of the β -phase, (Ta,Hf) , in the $\gamma + \beta$ field appears to increase with increasing hafnium content; however, the metallic matrix formed on cooling the composition in the $\gamma + \text{L}$ area is softer even though the hafnium content is greater than compositions in the $\gamma + \beta$ field. The γ -phase $(\text{Ta},\text{Hf})\text{C}_{1-x}$ in the $\gamma + \text{L}$ area is also softer than that in the $\gamma + \beta$ region.

DISCUSSION

On the basis of the previously described results, the phase boundaries shown in figure 2 were traced, and an isothermal section at 2050° C was constructed. The hafnium-rich corner of the diagram contains a liquid phase and the position of the phase boundaries were deduced primarily from the Ta-Hf and Hf-C binary systems and the observed deformation of compositions of high hafnium content due to liquid formation.

In general, the phase relations at 2050° C are similar to those at 1850° C except for the presence of the liquid phase. No phases other than those present in the binary systems were observed. The ζ -phase sometimes found in the binary Ta-C system and shown as a dotted area in the ternary system at 1850° C (fig. 1) was not detected at 2050° C. The solubility of carbon in the β -phase is about 2 to 3 atomic percent. The solubility of carbon in tantalum at 2050° C is given as about 2.2 atomic percent in reference 13. The transformation of the β -phase, (Ta,Hf) solid solution into β -Ta and α -Hf at the

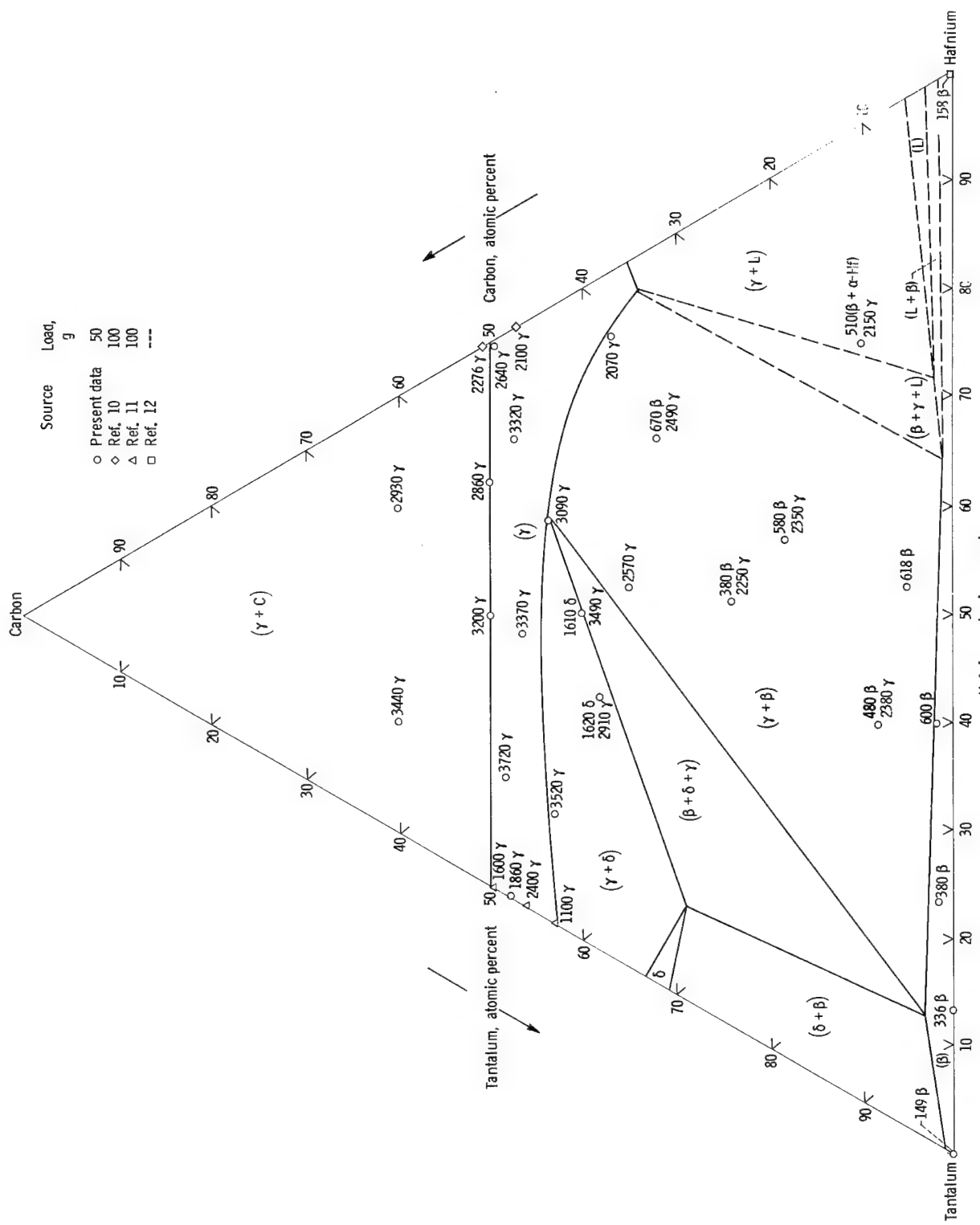


Figure 5. - Knoop hardness values of phases in tantalum-hafnium-carbon system.

cooling rate used in this study occurs only at high hafnium contents.

The $(\text{Ta},\text{Hf})_2\text{C}_{1-x}$ phase does not accept more than about 8 atomic percent hafnium at 2050°C . This occurs at the expense of tantalum and is accompanied by an increase in lattice parameter from $a_0 = 3.108$ angstroms, $c_0 = 4.948$ angstroms for Ta_2C to $a_0 = 3.120$ angstroms and $c_0 = 4.970$ angstroms for hafnium-saturated Ta_2C .

There is complete solid solubility between TaC and HfC , and the carbon content in the γ -phase, $(\text{Ta},\text{Hf})\text{C}_{1-x}$, may vary significantly. A hardness maximum appears to occur in the vicinity of 11 atomic percent hafnium, 41 atomic percent tantalum, and 48 atomic percent carbon (composition 30), which is near the compositions for which the highest melting point (ref. 1) and lowest vaporization rate (ref. 2) have been reported.

CONCLUSIONS

An isothermal cross section of the $\text{Ta}-\text{Hf}-\text{C}$ system at 2050°C was constructed from x-ray diffraction, chemical analysis, metallographic, and microhardness data. The complete solid solubility between TaC and HfC was verified. The lattice parameters of $(\text{Ta},\text{Hf})\text{C}_{1-x}$ solutions were determined. No phases other than those appearing in the three binary systems were observed. A liquid phase was found to be present in a large portion of the hafnium-rich corner. There is an exchange of hafnium for tantalum in the $\delta(\text{Ta},\text{Hf})_2\text{C}_{1-x}$ phase up to about 8 atomic percent. The lattice parameters increase correspondingly to $a_0 = 3.120$ angstroms and $c_0 = 4.970$ angstroms.

The ζ -phase, sometimes found in the $\text{Ta}-\text{C}$ system, was not observed in any of the compositions investigated at 2050°C . The limit of the $\gamma(\text{Ta},\text{Hf})\text{C}_{1-x} + \delta(\text{Ta},\text{Hf})_2\text{C}_{1-x}$ area extends to about 38 atomic percent hafnium, which agrees with that at 1850°C . The solubility of carbon in the $\beta(\text{Ta},\text{Hf})$ solid solution is about 2 to 3 atomic percent.

Lewis Research Center,
National Aeronautics and Space Administration,
Cleveland, Ohio, January 26, 1965.

REFERENCES

1. Agte, C.; and Alterthum, H.: Systems of High-Melting Carbides: Contributions to the Problem of Carbon Fusion. *Z. tech. Physik*, vol. 11, 1930, pp. 182-191.
2. Deadmore, Daniel L.: Vaporization of Tantalum-Carbide - Hafnium-Carbide Solid Solutions at 2500° to 3000°K . NASA TN D-2512, 1964.
3. Rudy, E.; and Nowotny, H.: Investigation of the Hafnium-Tantalum-Carbon System. *Monatsh. für Chem.*, vol. 94, no. 3, 1963, pp. 507-517.

4. Storms, E. K.: A Critical Review of Refractories. Pt. I. Selected Properties of Group 4a, 5a, and 6a Carbides. Rept. No. LAMS-2674, Los Alamos Sci. Lab., Feb. 1, 1962, p. 50.
5. Benesovsky, F.; and Rudy, E.: The Constitution of the Zirconium-Carbon and Hafnium-Carbon Systems. Planseeber. Pulvermet, vol. 8, 1960, pp. 66-71.
6. Kato, H.; Armantrout, C. E.; and Deardorff, D. K.: Hafnium Alloys. USBM-U-783, Quart. Met. Prog. Rept. No. 9, Oct. 1-Dec. 31, 1960, Albany Met. Res. Center, Dec. 1960, pp. 15-16.
7. Bowman, Allen L.: The Variation of Lattice Parameter with Carbon Content of Tantalum Carbide. J. Phys. Chem., vol. 65, no. 9, Sept. 1961, pp. 1596-1598.
8. Bittner, H.; and Goretzki, H.: Magnetic Researches on the Carbides TiC, ZrC, HfC, VC, NbC, and TaC. Monatsh. für Chem., vol. 93, 1962, pp. 1000-1004.
9. Santoro, G.; and Probst, H. B.: An Exploration of Microstructures in the Tantalum-Carbon System. Advances in X-Ray Analysis, Vol. 7, W. M. Mueller, G. Mallett, and M. Fay, eds., Plenum Press, 1963, pp. 126-135.
10. Adams, R. P.; and Beall, R. A.: Preparation and Evaluation of Fused Hafnium Carbide. Rept. No. BM-RI-6304, 1963. Bur. of Mines.
11. Santoro, Gilbert: Variation of Some Properties of Tantalum Carbide with Carbon Content. Trans. Met. Soc. AIME, vol. 227, Dec. 1963, pp. 1361-1368.
12. Litton, F. B.: Preparation and Some Properties of Hafnium Metal. J. Electrochem. Soc., vol. 98, 1951, pp. 488-494.
13. Ogden, H. R.; Schmidt, F. F.; and Bartlett, E. S.: The Solubility of Carbon in Tantalum. Trans. Met. Soc. AIME, vol. 227, Dec. 1963, pp. 1458-1460.

TABLE I. - CHEMICAL ANALYSIS OF
STARTING MATERIALS

Tantalum hydride	
Element	Weight percent
H	0.49
O	.072
N	.031
Si,W	0.005 - 0.05
Fe,Zr	0.01 - 0.10
Ti,Cu,Ni,V,Mn,Nb, Ca,Mg,Pb,Ba,K	<0.01
All other elements	All other elements not detected

Hafnium hydride	
Element	Weight percent
H	1.1
Zr	1.6
O	.02
N	.003
Fe	.025
C	.015
B,U,Cd	<.001
Al,Mo,Si,W,Cr,Pb, Ni,Na,Co,Mg,Sn, V,Ca,Cu,Mn,Ti	0.001 - 0.01

TABLE II. - COMPOSITION, PREPARATION, AND ROOM TEMPERATURE X-RAY DIFFRACTION DATA

Sample number	Composition, atomic percent	Tantalum	Hafnium	Composition, atomic percent	Number of phases detected by room-temperature x-ray diffraction	Phases present by room-temperature x-ray diffraction and lattice parameters ^a				Sample number	Composition, atomic percent	Method of preparation	Number of phases detected by room-temperature x-ray diffraction	Number of phases present by room-temperature x-ray diffraction and lattice parameters ^a		
						ρ (Ta, Hf)	α (Hf, Ta)	$5(\text{Ta}, \text{Hf})^2 \text{C}_{1-x}$	$\gamma(\text{Ta}, \text{Hf}) \text{C}_{1-x}$							
1	80	0	20	Sintered	2	3.306	N.D.	3.103	4.938	51	10	50.5	60	N.D. N.D.		
2	71	29	Sintered	2	3.306	N.D.	3.103	4.948	N.D.	52	47	55	52	3.126 N.D.		
3	64	36	Arc-melted	2	3.306	N.D.	3.103	4.948	N.D.	53	30	50	52	3.111 N.D.		
4	52	48	Hot pressed	1	3.309	N.D.	3.103	4.948	N.D.	54	30	50	52	3.111 N.D.		
5	51	49	Sintered	1	3.309	N.D.	3.103	4.948	N.D.	55	30	50	52	3.127 N.D.		
6	95.5	.5	10	Body centered cubic	2	3.309	N.L.	3.119	4.968	N.D.	56	42	23	35	3.120 N.D.	
7	93.8	.2	13.8	Body centered cubic	2	3.309	N.D.	3.119	4.953	N.D.	57	29.8	34.7	35.5	3.121 N.D.	
8	78.5	2.7	29.8	Body centered cubic	2	3.309	N.L.	3.119	4.953	N.D.	58	28.1	31.6	36.9	3.121 N.D.	
9	70.1	1.1	29.8	Body centered cubic	2	3.309	N.L.	3.109	4.942	N.D.	59	19.6	41.1	45.5	3.121 N.D.	
10	60.6	1.5	37.9	Body centered cubic	2	3.309	N.D.	3.108	4.942	4.414	60	12.8	37.8	49.5	3.121 N.D.	
11	55.6	1.7	42.7	Body centered cubic	2	3.309	N.L.	3.110	4.949	4.419	61	59.2	39.4	31.4	N.D. N.D.	
12	60	3	37	Body centered cubic	2	3.309	N.D.	3.116	4.953	4.419	62	30	40.5	30	3.126 N.D.	
13	73	5	22	Body centered cubic	2	3.309	N.D.	3.116	4.953	4.419	63	34.5	34.5	34.5	3.126 N.D.	
14	69	4	27	Body centered cubic	2	3.312	N.D.	3.122	4.971	N.D.	64	10	42.6	47.4	3.126 N.D.	
15	65.9	5.9	28.2	Body centered cubic	2	3.312	N.L.	3.114	4.950	N.D.	65	35	30	30	3.126 N.D.	
16	64	5.2	30.8	Body centered cubic	2	3.312	N.D.	3.111	4.945	N.L.	66	34	34	32	3.126 N.D.	
17	64.5	3.4	33.1	Body centered cubic	2	3.312	N.D.	3.107	4.946	4.457	67	29	31	31	3.126 N.D.	
18	60.7	5.4	33.9	Body centered cubic	2	3.312	N.L.	3.109	4.946	4.457	68	39.5	39.5	24	3.126 N.D.	
19	52.5	7.5	40	Body centered cubic	2	3.312	N.L.	3.109	4.946	4.457	69	38	38	33	3.126 N.D.	
20	87.9	7.8	4.3	Body centered cubic	2	3.316	N.L.	3.125	4.971	N.D.	70	20	44.1	34.5	3.126 N.D.	
21	91.1	9.4	9.5	Body centered cubic	2	3.316	N.L.	3.137	5.005	N.D.	71	52.3	42	5.7	N.L. N.L.	
22	64.1	9.4	28.1	Body centered cubic	2	3.316	N.L.	3.115	4.954	N.D.	72	56	36	36	3.126 N.L.	
23	75	9.0	29.1	Body centered cubic	2	3.316	N.D.	3.114	4.942	N.L.	73	34	48	37	3.126 N.L.	
24	61.3	7.2	31.5	Body centered cubic	2	3.316	N.D.	3.101	4.942	N.L.	74	15	37	37	3.126 N.L.	
25	57.7	6.6	35.7	Body centered cubic	2	3.321	N.D.	3.106	4.945	4.444	75	36.5	39.5	24	3.126 N.L.	
26	54.5	10.5	35	Body centered cubic	2	3.321	N.D.	3.129	4.971	4.504	76	5	48	47	3.126 N.L.	
27	65	10	25	Arc melted	2	3.321	N.D.	3.129	4.953	4.555	77	45	50	47	3.126 N.L.	
28	30	10	60	Arc melted	2	3.321	N.D.	3.129	4.459	4.504	78	24	49	26	3.126 N.L.	
29	49.3	10	40.7	Hot pressed	1	3.321	N.D.	3.129	4.442	4.504	79	24.5	49.5	26	3.126 N.L.	
30	41	11	48	Hot pressed	1	3.321	N.D.	3.129	4.442	4.504	80	17.5	50.5	32	3.126 N.L.	
31	46.7	9.9	43.4	Arc melted	1	3.321	N.D.	3.145	4.955	4.444	81	6	57	37	1 N.D. N.D.	
32	55	10.3	34.7	Sintered	2	3.321	N.L.	3.125	4.981	4.534	82	11.5	46.5	42	1 N.D. N.D.	
33	45	15	40	Sintered	2	3.321	N.L.	3.112	4.963	4.500	83	20	60	20	3.126 N.D.	
34	74	15.2	10.8	Sintered	2	3.319	N.L.	3.112	4.954	4.504	84	40	50	40	3.126 N.D.	
35	37	64	15.6	5	Arc melted	2	3.328	N.D.	3.156	4.956	4.556	85	7.5	67.5	25	3.126 N.D.
36	90	15.6	20.4	Sintered	2	3.328	N.L.	3.132	4.934	4.547	86	20	70	10	3.126 N.D.	
37	57	15.6	28	Sintered	2	3.328	N.L.	3.132	4.934	4.547	87	26	66	8	3.126 N.D.	
38	56	14	30	Sintered	2	3.328	N.L.	3.125	4.955	4.555	88	8.5	76.5	13	3.126 N.D.	
39	50	17	33	Sintered	2	3.328	N.L.	3.131	4.986	4.557	89	9	87	8.7	3.126 N.D.	
40	74	15.2	10.8	Sintered	2	3.319	N.L.	3.132	4.955	4.555	90	0	50.4	49.6	3.126 N.D.	
41	75.7	22.9	19.5	Arc melted	1	3.352	N.D.	3.310	4.955	4.556	91	0	56	42	3.126 N.D.	
42	61	20	46.4	Arc melted	1	3.352	N.D.	3.310	4.955	4.556	92	0	59	41	3.126 N.D.	
43	41.5	39.4	22.5	Sintered	2	3.346	N.D.	3.312	4.955	4.556	93	86	14	0	3.126 N.D.	
44	50	26	10	Sintered	2	3.346	N.D.	3.312	4.955	4.556	94	86	20	0	3.126 N.D.	
45	64	26	10	Sintered	2	3.346	N.D.	3.312	4.955	4.556	95	86	20	0	3.126 N.D.	
46	41.5	39.4	22.5	Sintered	2	3.346	N.D.	3.312	4.955	4.556	96	86	20	0	3.126 N.D.	
47	28.5	25.5	25.6	Arc melted	1	3.346	N.D.	3.312	4.955	4.556	97	86	20	0	3.126 N.D.	
48	43	24.7	27.7	Hot pressed	1	3.346	N.D.	3.312	4.955	4.556	98	86	20	0	3.126 N.D.	
49	43	24.7	27.7	Arc melted	1	3.346	N.D.	3.312	4.955	4.556	99	86	20	0	3.126 N.D.	
50	67.4	26.7	5.9	Sintered	2	3.361	N.D.	3.361	4.955	4.556	100	86	20	0	3.126 N.D.	

^a All lattice parameters are given in angstrom units, with a standard deviation of ± 0.005 .^b Phase was not detected by x-ray diffraction.

-

-

-

-

-

-

-

-

"The aeronautical and space activities of the United States shall be conducted so as to contribute . . . to the expansion of human knowledge of phenomena in the atmosphere and space. The Administration shall provide for the widest practicable and appropriate dissemination of information concerning its activities and the results thereof."

—NATIONAL AERONAUTICS AND SPACE ACT OF 1958

NASA SCIENTIFIC AND TECHNICAL PUBLICATIONS

TECHNICAL REPORTS: Scientific and technical information considered important, complete, and a lasting contribution to existing knowledge.

TECHNICAL NOTES: Information less broad in scope but nevertheless of importance as a contribution to existing knowledge.

TECHNICAL MEMORANDUMS: Information receiving limited distribution because of preliminary data, security classification, or other reasons.

CONTRACTOR REPORTS: Technical information generated in connection with a NASA contract or grant and released under NASA auspices.

TECHNICAL TRANSLATIONS: Information published in a foreign language considered to merit NASA distribution in English.

TECHNICAL REPRINTS: Information derived from NASA activities and initially published in the form of journal articles.

SPECIAL PUBLICATIONS: Information derived from or of value to NASA activities but not necessarily reporting the results of individual NASA-programmed scientific efforts. Publications include conference proceedings, monographs, data compilations, handbooks, sourcebooks, and special bibliographies.

Details on the availability of these publications may be obtained from:

SCIENTIFIC AND TECHNICAL INFORMATION DIVISION

NATIONAL AERONAUTICS AND SPACE ADMINISTRATION

Washington, D.C. 20546